

## Article

# Summer Dystrophic Criticalities of Non-Tidal Lagoons: The Case Study of a Mediterranean Lagoon

Mauro Lenzi <sup>1,\*</sup>  and Fabio Cianchi <sup>2</sup><sup>1</sup> Lagoon Ecology and Aquaculture Lagoon OPL s.a.r.l. v. G. Leopardi 9, 58015 Orbetello, Italy<sup>2</sup> World Wildlife Found Italy Foundation, v. Litoranea 35, 58011 Capalbio, Italy

\* Correspondence: lealab1@gmail.com

**Abstract:** Eutrophication determines algal blooms and the subsequent accumulation of organic matter in sediments, which, in turn, results in the dominance of anaerobic respiratory processes that release toxic gases. Dystrophy is a final dissipative moment that reduces the organic load in the sediment. A case of dystrophy occurring in the Burano lagoon (Tuscany, Italy) in 2021 is reported. The study examined the weather, physico-chemistry of the water, submerged vegetation and sediment labile organic matter. In spring, dissolved oxygen (DO) and pH showed high values, in an abundance of submerged vegetation, while low values had ammonium, nitrate and orthophosphate. In mid-August, as warm and moist sea breezes prevailed, hydrogen sulfide releases were produced, preceded by a sharp rise in ammonium and orthophosphate concentrations, which remained high until November. During dystrophy, DO varied between anoxia and oversaturation, the latter in Cyanobacteria blooms. Dystrophic waters evolved gradually due to microphytes blooms, which changed from Cyanobacteria, in August, to the Dinophyta *Alexandrium tamarense*, in September, and Bacillariophyta, in November. Sediment labile organic matter varied between 3% and 7%. *Ruppia spiralis* meadows suffered the total detachment of fronds and stems during the dystrophy and proved to be areas of accumulation of organic detritus, themselves sources of dystrophic phenomena.



**Citation:** Lenzi, M.; Cianchi, F. Summer Dystrophic Criticalities of Non-Tidal Lagoons: The Case Study of a Mediterranean Lagoon. *Diversity* **2022**, *14*, 771. <https://doi.org/10.3390/d14090771>

Academic Editors: Yulia I. Gubelit and Michael Wink

Received: 12 August 2022

Accepted: 15 September 2022

Published: 18 September 2022

**Publisher's Note:** MDPI stays neutral with regard to jurisdictional claims in published maps and institutional affiliations.



**Copyright:** © 2022 by the authors. Licensee MDPI, Basel, Switzerland. This article is an open access article distributed under the terms and conditions of the Creative Commons Attribution (CC BY) license (<https://creativecommons.org/licenses/by/4.0/>).

**Keywords:** non-tidal lagoon; lagoon dystrophy; eutrophication; macroalgal biomass; microphytes bloom; Burano lagoon

## 1. Occurrence of Dystrophic Phenomena in Non-Tidal Eutrophic Lagoons

Mediterranean lagoons, except for those in the North Adriatic, are non-tidal lagoons. Tidal ranges are, in fact, 20–30 cm, and only in the syzygial ones can 50 cm be reached. Therefore, they are environments with little exchange with the sea. Due to their morphology and structure, non-tidal lagoons are mesotrophic environment and tend to eutrophy. The consequences are all the more severe the lower the water exchange is, since the basin is more confined to the sea. Things went relatively well until the end of the 1960s, when summer environmental crises, consequences of mesotrophic/eutrophic conditions, occurred every 10 or even 15 years. Due to tourism and increased coastal strip anthropization, lagoon ecosystems have become hypereutrophic. The environmental situation degenerated more and more, and the time between crises has become shorter and shorter.

Eutrophication, understood as an increase in the bioavailability of the macronutrients nitrogen (N) and phosphorus (P) [1], involves intensive growth of opportunistic microphytes and macroalgae [2–6]. These blooms enrich the ecosystem with organic matter (OM), which is subject to first aerobic and then anaerobic bacterial aggression. Bacterial breakdowns return nutrients and allow further vegetative growth.

Non-tidal lagoons, due to their shallow depth, low water exchange, high light systems and “traps” for nutrients, tend to have high submerged vegetation developments. In their best condition, these are due to seagrass meadows. According to the conceptual model shown in Figure 1, OM enrichment causes instability and changes in plant stands,

establishing vegetation cycles with extremes ranging from low levels of sediment energy, e.g., after an environmental crisis, to high levels, just before the next crisis [7]. This view explains the significant temporal variations in the aquatic vegetation of mesotrophic and eutrophic lagoons and estuaries, in line with the broader picture of vegetation variations proposed by Duarte [8], for the transition from oligotrophic to eutrophic conditions in marine environments. The cycle involves a series of increasingly tolerant and opportunistic species. The amounts of OM and nutrients released by the sediment increase with the increase in plant biomass. As the sediment is enriched with OM, with the progressive increase in nutrient releases from the sediment, there is the growing prevalence of ammonium compared to nitrate (the dominant chemical species in which N is found is a selective factor for vegetation). For low values of OM in sediments, seagrasses are dominant; at the opposite extreme, in the growing eutrophic degradation of environmental conditions, Chlorophyta became dominant; between the two extremes, intermediate stages alternate, each of which has its own condition of OM, quantity of nutrient release, dominance of the various chemical species of N and atomic ratio N:P values [9].

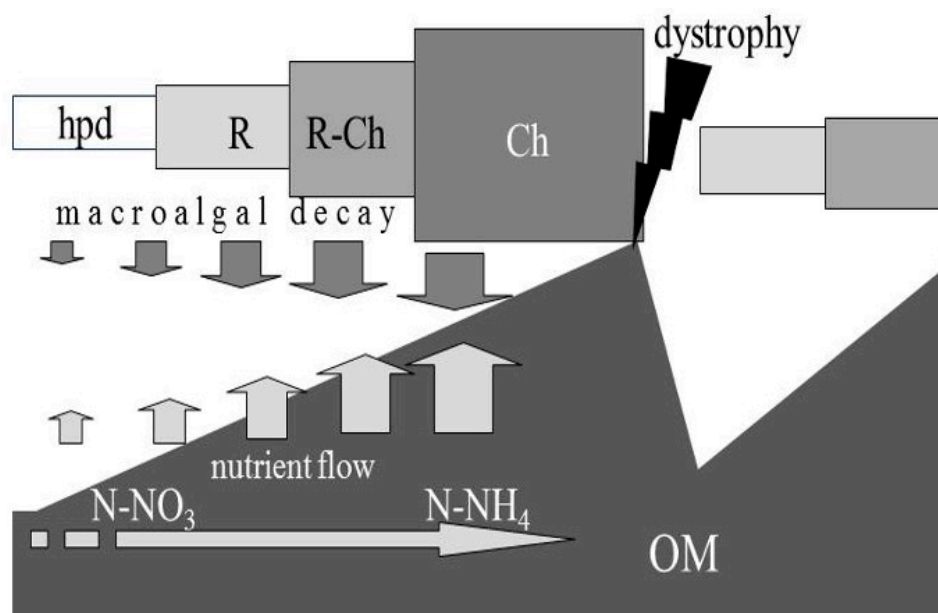


**Figure 1.** Release of nutrients from the sediment and their drift towards the dominance of ammonium as the sediment organic matter (OM) is increasing (arrow from left to right), and cycle/fluctuations of dominance/abundance of the species of the lagoon vegetation, as a result of accumulations and dissipation (dystrophy) of OM (OM, in dark in the lower part of the figure). The model expresses a cyclical trend that sees the conclusion of a vegetational condition following a dystrophic event and start of a new growth cycle immediately afterwards. The new start will come from one of the growth stages concerning the degree of dissipation. hpd, high biodiversity; R, Rhodophyceae; Ch, Chlorophyceae (from Lenzi et al. [9], modified).

Bacteria activity consumes oxygen and rapidly brings surface sediments into anaerobic conditions; this occurs faster and more markedly with rising temperatures between late spring and summer. Anaerobic processes occur first through the utilization of oxyhydroxides of  $\text{Fe}^{3+}$  and  $\text{Mn}^{4+}$  [10], as oxidants of organic matter, then through the respiration of nitrate ( $\text{NO}_3^-$ ), producing ammonia ( $\text{NH}_3$ ), and after through the respiration of sulphates ( $\text{SO}_4^{2-}$ ), producing hydrogen sulfide ( $\text{H}_2\text{S}$ ) and, more generally, volatile acid sulfides (AVS;  $\text{H}_2\text{S}$ ,  $\text{HS}^-$ ,  $\text{S}^{2-}$ ,  $\text{FeS}$ ) [11]. The sediment redox becomes increasingly negative. Each step in the anaerobic OM degradation results in the accumulation of increasingly reducing chemicals, and this drift makes it possible for new compounds to act as oxidants.

The process may remain confined to sediments or even affect the water column by releasing toxic gases,  $\text{NH}_3$  and  $\text{H}_2\text{S}$ , and other reducing components. The environment's

responses to the eutrophication consequences vary with the capacity of various ecosystems to buffer its effects [12]. Sediment rich in iron and manganese oxides–hydroxides offers a greater buffering capacity to AVS releases than sediment that is poor in them, which is more likely to compromise the water column [13].

These environmental criticalities, which in the popular French term are indicated as a whole *maläigue* (bad water), in Italian “*acquacce*” (bad water) or “*solfaia*” (sulfur bloom), are technically called dystrophy. This term would suggest that the lagoon environment moved from a condition of eutrophy to one of nutrient absence. Actually, it alludes to an alteration of nutrient cycles and the dysfunction of specific bacterial processes, such as nitrification. Finally, trophic alteration consists of the total removal, for a variable time, of dissolved oxygen. In contrast, the opposite occurs for nutrients, i.e., they become even more abundant, precisely due to the decay and anaerobic demolition of plant masses, particularly ammonium and orthophosphate ions. For simplicity’s sake, the phenomenon is often referred to as a sulfur bloom, which takes the most striking and obvious phenomenon of the release of hydrogen sulfide and its oxidation to sulfur as the cornerstone. Dystrophic phenomena are widespread in Mediterranean lagoons and have become increasingly frequent since the 1970s, in conjunction with eutrophication and increased human activities [14–17] (Figure 2).



**Figure 2.** Dystrophies in non-tidal lagoons of the Montpellier department (France). The slight green colouration is a development of Cyanobacteria; the lactescence is due to colloidal sulfur. Sentinel-2 image of 1 July 2022.

Dystrophic crisis is a dissipative process through which the ecosystem, which has reached unsustainable energy conditions, tends towards restoration. In essence, through dystrophic dissipation, the ecosystem eliminates the excess energy accumulated in the sediment as organic matter [9,16]. It blocks the process of species seriation and imposes a game-over and process turnover, starting again from zero, if the energy dissipation was very intense, or from an intermediate stage, if the dissipation was incomplete. Dystrophy is triggered, in this context, by an interrelation between the amount of OM accumulated and the environmental conditions.

The most severe dystrophies, capable of compromising the ecosystem by extensive fish die-off, occur through the concomitance of three factors: (1) high load of labile organic matter (LOM), (2) thermal raising ( $>25\text{ }^{\circ}\text{C}$ ), and (3) poor hydrodynamics ( $<3\text{--}4\text{ cm s}^{-1}$ ) (Figure 3).

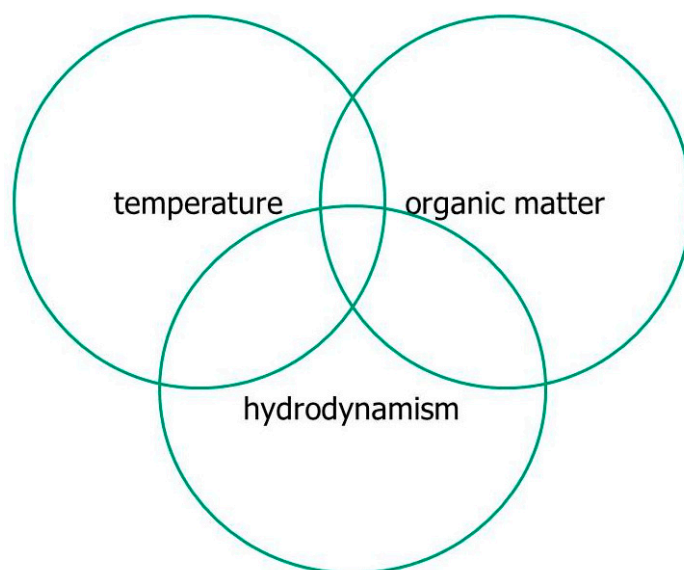


**Figure 3.** Interaction of the main factors that when combined can determine the onset of a dystrophic phenomenon. From Lenzi et al. [18], modified.

(1) A high LOM load is to be understood as the sedimentary deposits of organic detritus and macroalgal masses easily attacked by bacteria during temperature increase. Indeed, macroalgal masses capable of rapid decay can alone constitute the “fuel” for anaerobic bacteria. Most macroalgae consist largely of labile matter, except for some Chlorophyta, which have abundant amounts of cellulose macromolecules that are more resistant to bacterial aggression [19]. However, many others are rich in mucopolysaccharides and glucose components that are easily attacked. Seagrasses, on the other hand, have many cellulose fibres and consist mainly of refractory organic matter to bacterial attack.

(2) In order to make sulfate reducing bacteria (SRB) activity evident, which can always occur to a limited extent in the anoxic layer of the sediment, temperature rise must exceed 25 °C (Lenzi, laboratory test result, unpublished). The evidence consists of the formation of milky staining at the water/sediment interface. This colouration may be due to the development of bacteria of the genus *Beggiatoa*, which work by oxidizing sulfides and coating themselves with elemental sulfur [20], or by the formation of sulfur by the oxidation of AVS that have encountered the oxygen of the water column [21]. However, when temperatures rise further (>28 °C), sediment anoxia and SRB activity can affect the part of the water column close to the bottom. In that case, a milky formation is not observed, since the water mass is anoxic, so AVSs can enrich it. Disturbance due to boats or wind brings the water mass into suspension and remixes the AVS-rich anoxic layer with the overlying water mass in which oxygen is present, so the whole water column becomes milky in colour, making the phenomenon evident. If this occurs during the daytime, the criticality is mostly counteracted by atmospheric exchanges and photosynthesis of the still-viable vegetation. However, if it occurs during the night and early morning hours, it is accumulated to the respiratory processes, and the phenomenon can result in the death of the fish population [21].

(3) This last condition is the most critical and occurs under particular meteorological and hydrodynamic conditions, i.e., during windlessness, which results in water stagnation, or very humid sea winds. The high humidity prevents the exchange with the atmosphere of the heat accumulated in the waters during the day, increasing bacterial activity [21].

Paradoxically, the greater the depth of a hypereutrophic non-tidal lagoon, the more prone it is to criticality. Since there are no currents and the only movement of water masses is by wind, the greater the depth, the greater the wind intensity must be for the movement of water masses to reach the sediment, resuspend it, oxidize the organic detritus and stir up any stratification along the water column. Above 3 m, only rare atmospheric events of

high intensity can allow the superficial anoxic sediment to be stirred up. Rubegni et al. [22] demonstrated that, under hypereutrophic conditions, seagrasses succumb in static bottoms and are confined to the peripheral, shallower areas of the basin, which are more susceptible to wind disturbance, if these areas are not subject to the accumulation, still produced by the wind, of the macroalgal masses that would cause their suffocation.

Dystrophic conditions evolve more or less rapidly with weather conditions, i.e., the persistence of a lack of wind or humid winds or, otherwise, the onset of rain, dry landwinds and temperature decrease. The evolution of the conditions always passes through blooms of microphytes, such as purple or green sulfur bacteria, Cyanobacteria, Dinophyta, Bacillariophyta and more, until good oxidative conditions are re-established [21].

These complex dynamics stimulated the classification of different types of dystrophies. Hamon et al. [23] distinguished four types: (1) visible dystrophy, through surface white water, capable of producing significant mortality; (2) visible dystrophy that did not cause significant mortality; (3) bottom dystrophy instrumentally recorded; and (4) bottom dystrophy not recorded, but diagnosed a posteriori through other parameters (orthophosphate release). Lenzi [20] identified a number of types on empirical basis: (1) “silent dystrophy”, a dystrophic process that occurs gradually, without manifestation of important evidence, at most a milky-film from sulfur on the bottom; (2) “diffuse sulfur bloom”, when the activity of sulfate-reducing bacteria occurs gradually and AVS are dispersed in a relatively well-oxygenated water mass, forming a slight milky colouration with a diffuse turbidity; (3) “incipient dystrophy”, when, in a quiet situation, soluble sulfides rise from the bottom and diffuse into the hypoxia/anoxia zone ( $DO$  a little over  $0.1 \text{ mg L}^{-1}$ ; [24]) of the water column, in which case no elemental sulfur is formed and no colouration is felt: this situation can be evidenced chemically, e.g., by inputting a solution of  $\text{FeCl}_2$ ; (4) “daytime sulfur bloom”, when during the daytime, due to the action of a sufficiently strong wind or anthropogenic disturbance, the mixing of waters under incipient dystrophic conditions with waters with sufficient  $DO$  is produced, without any damage; (5) “sulfur bloom”, an evident, little extensive dystrophy with limited damage; (6) “dystrophic crisis”, an evident, very extensive dystrophy with significant fish mortality; (7) “sulfur bloom off”, when, after sulfur bloom has occurred, intense white/yellow colouration remains, but AVS is no longer detected, while  $DO$  may be  $>0$ ; and (8) “evolved sulfur bloom”, the condition of the water mass that had previously undergone dystrophy and now goes through a series of different transformation stages of various colourations, not always in the same sequence, due to physical (wind, temperature, lighting, etc.), chemical (atmospheric or photosynthetic oxygen) and biological factors (suspended particulate matter, sulfur cycle organisms, Cyanobacteria, Dinophyta, etc.).

Identifying these different types had the practical purpose of defining the stages of development and different conditions under which dystrophies can develop, to provide a framework to situate the observed situation and operate with any mitigation interventions.

Below, we report the results of the monitoring conducted in 2021, in a small coastal lagoon of the Tyrrhenian Sea, in the year in which a major dystrophic event occurred with fish die-off. The main contribution of this study was to have caught the dystrophic phenomenon as it was developing and to have been able to provide a before-and-after picture of the phenomenon, with the various stages of its evolution. Our objective has been to help better define the onset and evolution of these phenomena, which, although they are the end product of eutrophication, thus, essentially expected in highly eutrophic environments, remain poorly predictable, depending heavily on weather conditions.

### A case study

## 2. Materials and Methods

### 2.1. Study Area

The Burano lagoon, Italian State Nature Reserve, managed by WWF Italy, 9 km as the crow flies from the Orbetello lagoon, is situated on the south Tuscany coast (Italy). It is separated from the sea by a sandy bar consolidated by Mediterranean maquis. The lagoon

has a water surface area of about 170 ha and is elongated in form, extending parallel to the coast in a NW–SE direction (Figure 4), with an average depth of about 0.8 m. It receives water pumped from a large agricultural catchment (about 13.7 km<sup>2</sup>), through a network of canals that discharge into the lagoon through two main affluents, an eastern ditch and a western ditch (Figure 4). An outlet to the sea is periodically opened through the sand bar, which tends to close easily as soon as the lagoon water level has stabilized with the sea, to prevent flooding of the surrounding land. Salinity varies from 5 to 32, in an annual cycle, due to rainfall, evaporation and subdune seawater infiltration through the sand bar. The lagoon is hypereutrophic due to both inputs from the agricultural basin and effluent from the sewage treatment plant of a nearby urban center.

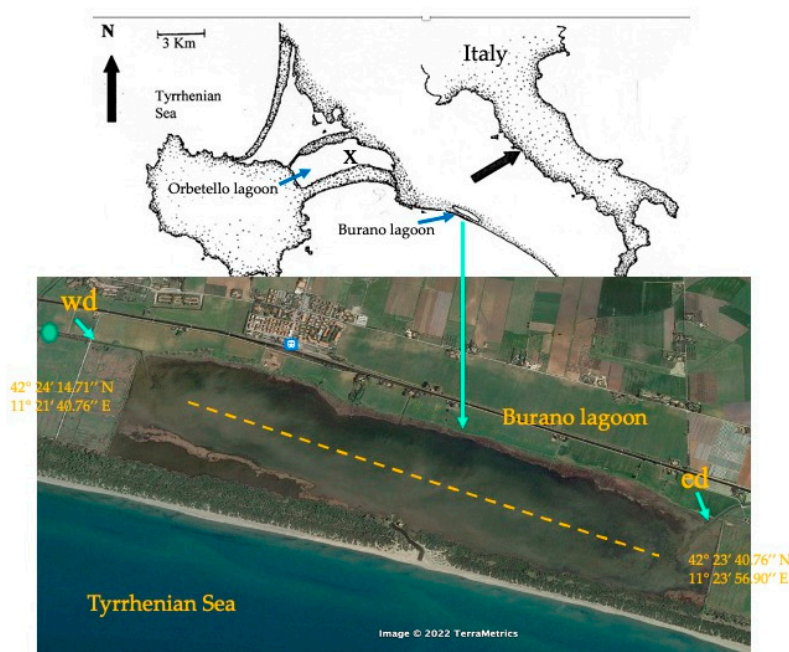


**Figure 4.** The Burano lagoon along the south Tuscany coast (Italy). In the center of the basin, in hatching, the transect for sampling and detection of the water physicochemical and nutrient variables, and sediment organic matter; wd, western ditch; ed, eastern ditch; dot, top left, sampling station for nutrient variables; x, in the eastern basin of the Orbetello lagoon, the meteorological control unit.

## 2.2. Monitoring 2021

Between May and November 2021, monitoring sponsored by WWF Italy was conducted to define the environmental status of the Burano lagoon (Tuscany, Italy; Figure 4). For this purpose, three ecosystem compartments were examined: the water column, sediment and vegetation.

### 2.2.1. Wind Direction/Intensity and Air Humidity

Wind direction, intensity and humidity were considered relevant for non-tidal lagoons. Indeed, in the absence of currents and tides, wind is the only force capable of producing hydrodynamic action. Depending on its intensity, it can resuspend the sediment, blocking the activity of anaerobic bacteria, and move floating macroalgal masses, favoring their accumulation. High air humidity can reduce heat and gas exchanges between the atmosphere and the water column. Data were obtained from the meteorological control unit in the eastern basin of the nearby Orbetello Lagoon (Figure 1).

### 2.2.2. Water Physicochemical Variables

Physicochemical measurements were conducted on 10 May, 15 July, 7 and 21 August, 15 September and 18 November, at six stations along a transect arranged on the basin's length (Figure 4), between 9:30 a.m. and 11:00 a.m. The variables were measured through

the use of portable instruments. Directly in situ, at approximately 20 cm from the surface, measurements of dissolved oxygen (DO), temperature (T, °C) (by OxyGuard Handy Mk III oxymeter), pH (by Delta OHM HD8705 electronic digital pH meter) and redox potential (Eh, mV; by Orion model 96-78-00 platinum electrode; the values were corrected to the normal hydrogen electrode,  $E_{h_{NHE}}$ ) were conducted. Nephelometric turbidity (nephelometric turbidity units, NTU) and salinity (s; expressed in practical salinity scale; ATAGO S/Mill refractometer) measurements were conducted 2–3 h after sampling, in the laboratory, on small water volumes collected in the field.

### 2.2.3. Dissolved Nutrients

Water sampling for dissolved nutrient determinations was conducted on 10 May, 7 August and 18 November, by taking 500 mL at about 20 cm below the surface at each of the six sampling stations arranged along the central transect; on 21 August, a water sample was also collected along the western adductor ditch (Figure 4). The samples were chilled on board and within two hours transferred to the laboratory. In the samples, filtered at 0.45  $\mu\text{m}$ , were determined: total dissolved nitrogen: total dissolved nitrogen (TDN), nitrate nitrogen (N-NO<sub>3</sub>), nitrous nitrogen (N-NO<sub>2</sub>), ammonia nitrogen (N-NH<sub>4</sub>), total dissolved phosphorus (TDP) and soluble orthophosphates (SRP). Analyses were conducted according to APAT IRSA-CNR [25], and the variables were expressed in  $\mu\text{M}$ . Dissolved inorganic nitrogen (DIN = N-NH<sub>4</sub> + N-NO<sub>2</sub> + N-NO<sub>3</sub>), dissolved organic nitrogen (DON = TDN – DIN), dissolved organic phosphorus (DOP = TDP – SRP) and DIN:SRP molar ratio were then calculated.

### 2.2.4. Sediment

In each monthly survey, nine sediment samples were collected, on 10 May, 7 August and 18 November, along the transect arranged along the length of the basin (Figure 4), using a horizontal coring sampler (Figure 5) capable of collecting sediment matter from the top 3–4 cm thick, according to Lenzi and Renzi [26]. Samples were refrigerated and then, in the laboratory, filtered with 1 mm mesh and dried at 75 °C to constant weight. Total organic matter (OM), labile organic matter (LOM) and refractory organic matter (ROM) were determined. Samples brought to constant weight were weighed, taken to an oven at 250 °C for 6 h, cooled to anhydrous conditions and weighed again. Finally, they were taken to an oven at 450 °C for 6 h and again cooled and weighed [27]. LOM was obtained by subtracting from the weight at 75 °C that was obtained at 250 °C. ROM was obtained by subtracting from the weight at 250 °C that was obtained at 450 °C. LOM and ROM were expressed as a percentage of constant weight at 75 °C. Finally, OM was calculated as the sum of the LOM and ROM values.

### 2.2.5. Macroalgae and Seagrass

Lists of seagrasses and macroalgae species and macroalgal biomass estimations were carried out on 10 May, 7 August, and 18 November. Biomass was conducted by collecting and weighing the algae within the conventional area of 3600 cm<sup>2</sup>, using a 60 × 60 cm box lowered to the point station. The material collected inside the box was drained for a few minutes and weighed directly in the field using portable electronic balance, with sensitivity  $\pm 0.5$  g. The data were then fed back to the unit area of 1 m<sup>2</sup> and expressed as kg wet weight m<sup>-2</sup> (kg<sub>WW</sub> m<sup>-2</sup>). Sampling points varied between 8 and 12 per survey, depending on the mat extent. Samples were taken within the macroalgal mats to establish their density, and the overall mean ( $\pm$ SD) was calculated.

Through the retrieval of satellite images as coincident as possible with the sampling date (obtained from the Land-Viewer website, EOS DATA ANALYTICS, USGS/NASA, for the Landsat-8 and Sentinel-2 satellites), the extent of macroalgal mats was calculated using Fiji software [28]. The macroalgal coverage related to the extent of the area in question provided the total coverage:

$$EM \times A^{-1} = CT$$

where EM is the macroalgal extent, A is the total basin extent, and CT is the total macroalgal coverage over the basin extent.



**Figure 5.** Horizontal coring instrument for collecting 60 mL of surface sediment (3–4 cm thick). After positioning the instrument's base on the bottom, sending the messenger (vertically arranged metal block) triggers the spring that drags the syringe along the horizontal path at the instrument's base, collecting the sediment material.

Standing crop (SC), that is, the algal mass present in the lagoon surface during the survey, was calculated by applying the following equation:

$$SC = b \times CT \times A \times 1000^{-1}$$

where SC is the standing crop expressed in tonnes wet weight ( $T_{WW}$ ); b, the average biomass, obtained from field surveys, is expressed in  $kg_{WW} m^{-2}$ ; A, the basin area, is expressed in  $m^2$ ; and  $1000^{-1}$  is the factor to bring the final value to tonnes.

The equation is simplified by substituting CT for its estimated ratio:

$$SC = b \times EM \times 1000^{-1}$$

The available estimates of macroalgal SCs conducted in February 2018 and March 2019 were also considered, for which the same estimation criteria had been used.

Macroalgae were determined by Coppejans [29] and Burrows [30] and, for taxonomic updates, by WoRMS [31]. For seagrass, the species was named according to the revision of Ito et al. [32]. Determinations were made with microscopes Zeiss 47 50 22 and Wetzlar GMBH Leitz.

#### 2.2.6. Microphyte Blooms

Microphyte development was followed on 10 May, 15 July, 7, 21 August, 15 September and 18 November, only where bloom conditions were observed. Five 100 mL samples were collected per bloom and refrigerated in the field. In order to identify dominant taxa, determinations were made with microscope Wetzlar GMBH Leitz, according to ICRAM [33] and ISPRA [34]. Bloom intensity was assessed in the field with Secchi's disk.

### 2.3. Statistical Analysis

One-way ANOVAs were performed for  $\text{N-NH}_4^+$ ,  $\text{N-NO}_3^-$ , TDN, SRP, LOM and ROM, to detect significant differences between the three months of sampling. Cochran's C-test was used before each ANOVA analysis to check for homogeneity of variance and eventually operate with data transformation [35]. The Student Newman Keuls (SNK) post hoc test was used for a posteriori multiple comparisons of means, to see which specific pairs of means differ. Significant effects were considered for  $p < 0.05$ . These tests were performed with Statistica 10.0 software package.

For physicochemical variables, Kruskal–Wallis (KW) non-parametric test was used to detect differences at each time. Dunn's test (with Benjamini–Hochberg correction) was performed for pairwise multiple comparisons. Stata-17 software was used.

## 3. Results

### 3.1. Wind Direction/Intensity and Air Humidity

For this study, we report only the wind direction/intensity and air humidity during August, around the middle of which the dystrophy became evident.

Humid sea winds from the ESE, SE and S affected 42% of the records that were recorded by the anemographic station, with hourly frequency (744 records). The sea-wind records were concentrated without interruption on days 6, 7, 8, 9, 10, 16, 23, 24 and 27.

Winds  $> 8 \text{ m s}^{-1}$  capable of moving surface sediment were limited to 6.4% of the total records (744), with 50% concentrated in the first six days of the month, while winds  $< 4 \text{ m s}^{-1}$  prevailed. In 239 records between 6 and 15 August, the wind of intensity  $> 7 \text{ m s}^{-1}$  was 5%, with prevailing windlessness and intensity  $< 4 \text{ m s}^{-1}$ .

Air humidity between 7 and 12 August was  $84 \pm 7\%$  (127 records), and, between the days 15 and 23, it was  $80 \pm 6\%$  (188 records).

### 3.2. Water Physicochemical Variables

In Table 1, DO, pH, T,  $\text{Eh}_{\text{NHE}}$ , s and NTU mean ( $\pm$ SD) values, obtained between May and November 2021, are reported.

**Table 1.** Means ( $\pm$  SD) of physicochemical variables measured in the Burano lagoon between May and November 2021, at six stations arranged in a central transect along the basin's length. Dissolved oxygen (DO, in  $\text{mg L}^{-1}$ , range and percentage of saturation), temperature (T,  $^\circ\text{C}$ ), pH, redox potential ( $\text{Eh}_{\text{NHE}}$ , in mV), salinity (s, practical salinity scale) and nephelometric turbidity units (NTU).

	DO			T	pH	$\text{Eh}_{\text{NHE}}$	S	NTU
	$\text{mg L}^{-1}$	Range $\text{mg L}^{-1}$	%	$^\circ\text{C}$		mV		
10 May	$7.38 \pm 0.42$	7.06–7.98	$102 \pm 7$	$21.1 \pm 0.26$	$8.75 \pm 0.16$	$245 \pm 25$	$22 \pm 0.5$	$9 \pm 4$
15 July	$4.73 \pm 0.56$	4.11–5.47	$72 \pm 9$	$26.6 \pm 0.24$	$8.57 \pm 0.23$	$210 \pm 7$	$26 \pm 0.5$	$1 \pm 0.1$
7 August	$5.88 \pm 1.81$	3.27–10.30	$92 \pm 28$	$27.6 \pm 0.33$	$8.66 \pm 0.23$	$217 \pm 10$	$28 \pm 0.8$	$8 \pm 4$
21 August	$1.98 \pm 3.32$	0.00–10.40		$29.3 \pm 0.47$	$8.01 \pm 0.62$	$-21 \pm 53$	$30 \pm 0.5$	$44 \pm 18$
15 September	$7.78 \pm 2.88$	5.00–12.60	$110 \pm 40$	$23.0 \pm 0.33$	$8.56 \pm 0.22$	$215 \pm 7$	$33 \pm 0.9$	$36 \pm 16$
18 November	$4.12 \pm 0.44$	3.23–4.62	$49 \pm 6$	$13.9 \pm 0.24$	$8.04 \pm 0.14$	$242 \pm 40$	$26 \pm 0.5$	$27 \pm 3$

In May, DO values ranged around saturation, pH was higher than 8.60 and salinity was around 22. The mean ( $\pm$  SD) of the  $\text{Eh}_{\text{NHE}}$  values was  $245 \pm 25 \text{ mV}$ , and the median was  $257 \text{ mV}$ . Relatively high values of nephelometric turbidity (NTU) were measured.

Between July and 7 August, DO values fluctuated between  $3 \text{ mg L}^{-1}$  and  $10 \text{ mg L}^{-1}$ , with mean ( $\pm$ SD) for the entire period of  $5.59 \pm 1.67 \text{ mg L}^{-1}$  and median of  $5.46 \text{ mg L}^{-1}$ , showing some areas subject to intense respiratory activity and others to high photosynthetic activity. pH maintained high values with a peak of 9.17, in areas with high DO values. On 7 August, the salinity increased to 28, significantly higher than in May ( $p = 0.007$ ). The redox potential value was slightly lower than in May; it averaged  $215 \pm 10 \text{ mV}$  between July and

August 7, with a median of 219 mV. NTU increased in July and returned to May values on 7 August. Temperature on 7 August was significantly higher than in May ( $p = 0.007$ ).

The 21 August survey was conducted due to the development of an extensive dystrophic event. DO values fluctuated spatially between total anoxia, 0 mg L<sup>-1</sup>, and supersaturation, with peak of 10.4 mg L<sup>-1</sup>. Data differed significantly with those of May, 7 August and September ( $p < 0.006$ ). Temperature exceeded 29 °C and was significantly higher than in May, September and November ( $p < 0.005$ ). Salinity reached 30, differing significantly from May and November ( $p < 0.007$ ). pH varied spatially between 7.00 and 8.36. NTU values resulted significantly higher than those in May ( $p < 0.050$ ), July ( $p < 0.000$ ), 7 August and November ( $p < 0.010$ ). Eh<sub>NHE</sub> values varied between 72 and -82 mV and was resulted significantly lower than in May, on 7 August and in September ( $p < 0.000$ ).

In September, sharp rises in DO and pH throughout the basin were measured. DO data were significantly different from those of 21 August ( $p < 0.000$ ). Eh<sub>NHE</sub> recovered to July values. Salinity manifested a further increase and differed significantly from May, July and November ( $p < 0.002$ ). NTU values remained steadily high, significantly higher than in May, in July, on 7 August and in November ( $p < 0.05$ ). Temperatures fell below 25 °C.

In November, DO saturation was between 39% and 54%, with the lowest values in the western sector. DO data differed significantly with those of May and September ( $p < 0.009$ ). pH ranged between 7.8 and 8.2 and was significantly different than in all the others surveys ( $p < 0.010$ ). NTU was still very high, especially in the western area, but significantly lower than on 21 August and in September ( $p < 0.020$ ). Eh recovered, but the values were still significantly different from those in May ( $p < 0.003$ ), remaining lower in the western part of the basin. Temperature was significantly lower than in July and on 7 and 21 August ( $p < 0.008$ ).

### 3.3. Dissolved Nutrients

Table 2 shows the means of dissolved nutrient values in the samples collected on 10 May, 7 August and 18 November 2021.

**Table 2.** Means ( $\pm$ SD) of nutrient variables expressed in  $\mu$ M, DIN:SRP molar ratio, among water samples collected monthly at six stations arranged in a central transect along the length of the basin, and values of one sample collected on 21 August, in the western ditch (wd, Figure 4). Ammonia nitrogen, N-NH<sub>4</sub>; nitrous nitrogen, N-NO<sub>2</sub>; nitrate nitrogen, N-NO<sub>3</sub>; dissolved inorganic nitrogen, DIN; dissolved organic nitrogen, DON; total dissolved nitrogen, TDN; soluble reactive phosphorus, SRP; dissolved organic phosphorus, DOP; total dissolved phosphorus, TDP.

	N-NH <sub>4</sub>	N-NO <sub>2</sub>	N-NO <sub>3</sub>	DIN	DON	TDN	SRP	DOP	TDP	DIN:SRP
10 May	0.07 $\pm$ 0	0.1 $\pm$ 0.1	34 $\pm$ 5	34 $\pm$ 5	253 $\pm$ 43	287 $\pm$ 43	0.43 $\pm$ 0.10	0.5 $\pm$ 0.1	1.00 $\pm$ 0.15	81 $\pm$ 14
7 August	111 $\pm$ 31	0.3 $\pm$ 0.1	30 $\pm$ 19	141 $\pm$ 25	295 $\pm$ 138	436 $\pm$ 133	1.10 $\pm$ 0.90	0.4 $\pm$ 0.2	1.50 $\pm$ 1.00	1818 $\pm$ 2432
21 August	1.43	0.1	557	559	56	614	0	0	0	0
18 November	143 $\pm$ 20	2.0 $\pm$ 0.9	56 $\pm$ 5	201 $\pm$ 23	207 $\pm$ 95	408 $\pm$ 108	1.90 $\pm$ 0.60	0.6 $\pm$ 0.2	2.50 $\pm$ 0.60	121 $\pm$ 54

In May, dissolved nutrients showed the eutrophic condition typical of this basin, with DIN between 30 and 40  $\mu$ M, consisting almost entirely of N-NO<sub>3</sub>, and SRP was between 0.3 and 0.5  $\mu$ M. DON values were also high. The DIN:SRP atomic ratio ranged between 60 and 90.

In the first week of August, the situation appeared profoundly different. Ammonium values ranged from 81  $\mu$ M and 145  $\mu$ M, exceeding the May values by 2000 times ( $p < 0.001$ ). Nitrous nitrogen increased 6 to 10 times more than in May, and nitrate nitrogen values did not vary significantly from those in May. From May to 7 August, TDN increased by about 52%, although the differences between the two months were not significant because of the variability of the data. SRP increased by three to five times compared with May for the western and central zones, while in the eastern zone it decreased. Among all the data, the differences between the two months were not significant. The situation along the western ditch (Figure 4) that conveys freshwater was very different (Table 2): waters were very loaded with N-NO<sub>3</sub>, while N-NH<sub>4</sub> was scarcely present, and SRP was undetectable.

In November, ammonium values were still higher, significantly higher than in May ( $p < 0.001$ ) and August ( $p < 0.05$ ). Nitrates were also significantly higher in November than in August and May ( $p < 0.01$ ). TDN was also higher, but not significantly. SRP showed higher values between the central and eastern areas, and, overall, the data were significantly higher than in May ( $p < 0.01$ ) but not compared to August ( $p > 0.05$ ). The DIN:SRP ratio also maintained high values.

### 3.4. Sediment Organic Matter

The percentage values of total organic matter (OM), labile organic matter (LOM) and refractory organic matter (ROM) present in the sediment collected on 10 May, 7 August and 18 November 2021 are shown in Table 3.

**Table 3.** Percentages (mean among nine values  $\pm$  SD) of labile organic matter (LOM), refractory organic matter (ROM), and total organic matter (OM) compared to the sediment brought to constant weight at 75 °C from samples collected at Burano between May and November 2021, along a central transect arranged along the length of the basin.

	LOM %	ROM %	OM %
10 May	4.95 $\pm$ 0.72	5.69 $\pm$ 0.86	10.64 $\pm$ 1.55
7 August	5.92 $\pm$ 1.64	7.06 $\pm$ 1.65	12.98 $\pm$ 3.26
18 November	6.36 $\pm$ 0.88	7.72 $\pm$ 0.29	14.08 $\pm$ 0.72

LOM and ROM increased by about 19.60% and 24.10% between 10 May and 7 August, respectively, although for LOM the results were not significantly different, whereas they were for ROM ( $p < 0.01$ ). The values then further increased significantly between 10 May and 18 November, by 28.48% and 35.68%, for LOM ( $p < 0.05$ ) and ROM ( $p < 0.01$ ), respectively. Data were also significantly different between 18 November and 7 August ( $p < 0.05$ ) for LOM but not for ROM.

### 3.5. Submerged Vegetation

The estimation of the extent of the lagoon conducted with the Fiji program on the Sentinel-2 satellite image provided a total basin value of 176.7 hectares, in which salt marshes were also considered.

Sentinel-2 satellite images of 15 February 2018, 14 March 2019 and 8 May and 6 August, 2021 were used for the vegetation estimation of February 2018, March 2019 and May 10 and 7 August 2021, respectively. It was not possible to make the November estimate with the Fiji program due to the intense microphytes bloom that did not allow the satellite image to be used.

In May, from field surveys, no extensive mats of the macroalgae were observed, in contrast to past years when the Chlorophyta *Chaetomorpha linum* (O.F. Müller) Kützing accumulated with high densities, especially in the western part of the basin. Instead, a not very dense mélange was observed between the two dominant macroalgal species, *C. linum* and the Rhodophyta Ceramiales *Lophosiphonia obscura* (C. Agardh) Falkenberg, which alternated with the extensive patches of the seagrass *Ruppia spiralis* L. *C. linum* turned out to be more concentrated along the continental coastal belt of the western part of the basin. *L. obscura* was distributed everywhere in the basin, which was also often mixed with *Ceramium codii*, but with modest bottom cover densities and mats thicknesses not exceeding 2–4 cm.

The total biomass of macroalgal mats was found to be 1.251 kg m<sup>-2</sup>; plant cover (macroalgae and seagrass) was estimated at 105 ha, 59.4% of the basin area. *R. spiralis* was estimated to cover about 52 ha, 29% of the basin, and macroalgae 53.4 ha, 30% of the basin. Macroalgal standing crop (SC) was about 668 tonnes.

On 7 August, there was a sharp decrease in macroalgal biomass. It was distributed in small patches in the voids of the meadows and near the continental shoreline, where rotting masses of *C. linum* and *L. obscura* had accumulated. Macroalgal mats in good vegetative

condition did not exceed 10 ha coverage of the basin area, with 48 tonnes of SC. The average among all biomass data was  $0.548 \text{ kg m}^{-2}$ .

On the contrary, between 10 May and 7 August, the extent of the meadows increased to about 87.3 ha.

On 15 September, during monitoring of physicochemical variables, total decay of the submerged vegetation was observed, including an early detachment of the fronds and stems of *R. spiralis*.

On 14 November, submerged vegetation was almost absent: small clumps of *R. spiralis*, especially near the sandy bar, were mixed with the sparse presence of *C. linum*. The presence of decaying material mixed with detached seagrass fronds was abundant. Estimation with the satellite image and Fiji program was not possible due to high turbidity, while, through the sampling frame, the bottom was always found to be devoid of viable vegetation. Therefore, macroalgal masses in good vegetative state were considered negligible in terms of biomass and SC.

SCs and floristic lists, for May, August and November 2021, are given in Table 4 and Table 5, respectively. The number of species was low with only six occurrences, including one seagrass species. The Chlorophyta numerically prevailed, and all macroalgal species, except *C. codii*, are to be considered opportunistic species, able to exploit the hypereutrophic condition of the basin.

**Table 4.** Standing crops (SC) of macroalgae, expressed in tonnes wet weight ( $T_{WW}$ ), present in the Burano lagoon, in February 2018, March 2019 and May, August and November 2021. Standing crops were calculated through the extension of mats by Fiji program (except November) and estimation of macroalgal biomass ( $b$ , in  $\text{kg}_{WW} \text{ m}^{-2}$ ) was conducted in the field directly on the mats. neg., negligible.

	SC
February 2018	2520
March 2019	1970
10 May 2021	668
7 August 2021	48
18 November 2021	neg.

**Table 5.** Floristic list of submerged vegetation species observed between May and November 2021 in the Burano lagoon.

		May	August	November
Chlorophyta	<i>Chaetomorpha linum</i>	x	x	x
Chlorophyta	<i>Cladophora vagabunda</i>		x	
Chlorophyta	<i>Ulva intestinalis</i>	x	x	
Rhodophyta	<i>Lophosiphonia obscura</i>	x	x	
Rhodophyta	<i>Ceramium codii</i>	x		
Magnoliophyta	<i>Ruppia spiralis</i>	x	x	x

### 3.6. Blooms of Microphytes and Water Colourations

Blooms of Dinophyceae (undetermined) were observed in isolated patches, on 7 August. The Secchi disk disappeared between  $-40$  and  $-60$  cm from the surface, in the dark brown water. In mid-August, in the midst of dystrophy, the white/yellow colouration due to colloidal sulfur was mixed with brown waters laden with bacteria, Dinophyceae and very dark micro- and nanoparticulate (probably due to the formation of FeS within) (Figure 6). In the west area of the basin, intense blooms of Cyanobacteria (undetermined, Synecococcus-like) were observed to prevail with intense green water colouration, with a maximum of light extinction at Secchi disk at  $-20$  cm. In September, the entire lagoon basin was affected by an intense bloom of the Dinophyta *Alexandrium tamarense* (Lebour) Balech, with a loss of visibility of the Secchi disk at  $-20$  cm. In November, the basin was still affected by intense turbidity due to blooms of microphytes, sustained by bacterioplankton

and Bacillariophyceae, pennate and centric diatoms (numerous species, not determined). Loss of visibility of the Secchi disk was between  $-30$  and  $-40$  cm.



**Figure 6.** The Burano lagoon. Photos taken with drone on 16–18 August 2021. Top left image, extensive dystrophic phenomenon along the continental shoreline of the basin. The dark mottled strip, near the coast, consists of seagrass patches (R arrow); the yellow colour is produced by colloidal sulfur originating from oxidation of hydrogen sulfide released during the bacterial sulfate-reduction process (S arrow); the brown colour, more central, is the mixing of microphytic blooms, bacterioplankton and nanoparticulate with colloidal sulfur (S&M/B arrow). Top right image, detail of the area affected by dystrophy. Lower left image, extensive dystrophic phenomenon that affected the extreme eastern part of the basin. Milkiness due to colloidal sulfur; just above, in yellow, colloidal sulfur and mixing with brown water. Lower right image, sulfur blooms emerging (in yellow, S arrows) from seagrass patches (in very dark colour, R arrows); the dark waters around are borne by bacterial developments, Dinophyta and suspended particulates (D-sp arrows).

#### 4. Discussion

##### 4.1. Water Physicochemical Variables

In May, the values of the physicochemical variables (Table 1) were as expected during the spring season, with high values of DO and pH, due to high plant biomass, for both macroalgae and seagrass. Salinity had a good value for fish and infauna populations and was able to retain more DO than 37 of the nearby sea. Relatively low, compared with the high DO values, were the redox potential values ( $E_{h_{NHE}}$ ). This could mean that reducing components had accumulated in the water column, due to releases by bacterial activity on the sediment and suspended nanoparticulate. The high presence of nanoparticulate was

evidenced by the relatively high values of NTU (Table 1), especially in the western zone, where DO values were lower than in other basin areas.

Spatial variability of DO, observed in the first week of August, is common in shallow non-tidal eutrophic lagoons, on which much can be affected by increases in temperature and salinity; in our case, reached peaks of salinity and temperature around 29 and 28 °C, respectively (Table 1), lowering DO saturation values to about 6 mg L<sup>-1</sup>. Salinity increased due to evaporation and reduced freshwater input from the two tributary ditches flowing to the western and eastern ends of the basin.

In the second half of August, during dystrophy, blooms of Cyanobacteria, distributed in patches, especially in the western area, resulted in localized increases in DO, while much of the basin surface was found to be hypoxic, around 0.8 mg L<sup>-1</sup>, with values not exceeding 2.5 mg L<sup>-1</sup> (Table 1).

In September, the *Alexandrium tamarense* bloom determined increases in DO and pH, but Eh<sub>NHE</sub> values were still well below what they should be for a basin with a dominance of autotrophs over heterotrophs, while NTU values were very high due to the bloom. Temperatures below 25 °C ruled out that major dystrophic activity could still occur.

In November, the environmental condition had not yet recovered (Table 1). Turbidity stayed high from the microphytes bloom. Low redox values in the western section of the basin indicated the permanence of dissolved reducing chemicals in the water column.

As the dystrophy in the second half of August affected the central and eastern areas more than the western area, and the former two showed, in November, a better recovery than the western, it can be assumed that the dystrophy in the central and eastern areas dissipated much of the organic “fuel” that sustained the dystrophy, allowing these areas to restart with better environmental conditions than the western area.

#### 4.2. Dissolved Nutrients

The low presence in May of N-NH<sub>4</sub><sup>+</sup> and N-NO<sub>2</sub><sup>-</sup> was probably favored by the relatively high, evenly distributed DO values (Table 1), which would have favored a rapid nitrification process. The high DON value was a typical condition of eutrophic lagoons with low water turnover, which accumulate dissolved organic matter (DOM) due to decay of plant masses and cell lysis, releasing soluble macromolecules. DIN:SRP expressed P-limitation condition. DIN:SRP 16 and 30 are considered physiologically best for phytoplankton and macroalgae, respectively, because they coincide with the average atomic ratios of the internal content of the two macronutrients [36,37]. However, the estimated values in the Burano lagoon do not express a true P-limitation, because the two nutrient components were both very abundant, albeit in strong disequilibrium, in a ratio that favored nitrogen. This is quite typical of eutrophication from inputs outside the ecosystem, as was later confirmed by water analysis conducted in August along the western ditch (Table 2). It is most likely that a DIN input came from the civil wastewater, which is conveyed with the waters of the ditch that drains into the western side of the basin. Municipal wastewaters, even purified ones, maintain a high nitrogen load, while P-PO<sub>4</sub><sup>3-</sup>, over a sufficiently long path, as in the case of the adductor ditch, gradually leaves the water column, precipitating as insoluble salts of calcium and magnesium. The nutrient values determined were sufficient to support high macroalgae or microphytes blooms.

In the first week of August, high ammonium values could produce at chemical equilibrium a concentration of undissociated ammonia (NH<sub>3</sub>) well above 1.2 μM, which is the safe limit for fauna. In fact, at pH 7.8 and 25 °C, this limit would already be reached at an ammonium concentration of about 37 μM [38]. More importantly, the nitrification process had been greatly reduced, given the high ammonium and nitrite values, and the nitrate values did not vary from those in May. The bacterial ammonification process likely increased in the sediment, and, consequently, ammonium was released into the water column. Indeed, a large deviation of oxygen from 100% saturation was detected during that period, which means the system had an insufficient capacity to oxidize reduced nitrogen, and, more generally, DOM in the water column.

In some of the areas, the anoxia and decomposition of sediment OM were likely the cause of SRP releases, through the sulfate breathing process and the release of phosphates from the reduction of Fe<sup>III</sup> (oxyhydroxides) and sequestration of Fe<sup>II</sup> by sulfides [10,39]. The SRP decrease in the eastern area, given the high DO value in its some zones (Table 1; 10 mg L<sup>-1</sup>), may be attributed to uptake by the microphytes bloom.

The high N-NO<sub>3</sub><sup>-</sup> value and very low concentrations of N-NH<sub>4</sub><sup>+</sup> and SRP along the western ditch that conveys freshwater mean that external N inputs could have been very important, depending on the water flow, but ammonification, low nitrifying activity and orthophosphate release were endogenous phenomena of the lagoon.

In November, N-NH<sub>4</sub><sup>+</sup> releases continued throughout the basin, probably due to bacterial ammonification activity of past and more recently decayed OM. High N-NH<sub>4</sub><sup>+</sup> and N-NO<sub>2</sub><sup>-</sup> values mean that the nitrification process was still fatiguing because of the overall oxidative state, which was likely still too low for this process. Environmental conditions remained critical, albeit in a nondystrophic setting, mainly due to the lowering of the temperature.

In this monitoring experience, we observed the change in terms of nutrients between a spring phase that did not portend criticality and the phase in which rising temperatures and stagnant waters allowed anaerobic processes to take over, such that they also involved the water column. This phase of the onset of criticality was characterized of a strong increase in the ammonium ion and, subordinately, the nitrous and orthophosphate ions. Ammonium nitrogen appears as an indicator of the onset of criticality, which may evolve into dystrophy with the prevalence of the sulfate reduction process.

#### 4.3. Sediment Organic Matter

The OM increases in sediments between May and November can be attributed first to the macroalgal decay and then to the decay of seagrass fronds, caused in advance by the dystrophic crisis. ROM increases can be attributed mainly to seagrass.

However, LOM values were not found to be very high. They were below the value that was adopted in the Environmental Safety Plan for the Management of the Orbetello Lagoon [40], which was based on the data collected in 2015 in that lagoon, when a dystrophy occurred. Through that experience, a LOM value of 8% (on dried sediment at constant weight) was taken as a “threshold of attention”, above which the risk of dystrophic crisis can be high if accompanied by temperature > 29 °C and DO < 2 mg L<sup>-1</sup>. This is undoubtedly an essential reference, but it is still very approximate. It neglects the masses of macroalgal species that can collapse rapidly under critical conditions and constitute immediate new energy for SRB, the dissolved organic matter (DOM) and the nature of LOM itself. LOM can produce different effects if it consists mainly of hydrocarbons, lipids or proteins [41,42].

#### 4.4. Submerged Vegetation

In the Tyrrhenian lagoons, the highest macroalgal standing crop is reached in May. The Sc of 10 May in the Burano lagoon was relatively low, with only 668 tonnes (1.251 kg m<sup>-2</sup> in 53.4 ha on 176.7 ha). These in 7 August were reduced to 48 tonnes, with probable decay in sediments of more than 600 tonnes, an average macroalgal decay of 1.124 kg m<sup>-2</sup> for the areas occupied by mats. The Sc of May 2021 was lower than that of February 2018 and March 2019, which reached 2520 tonnes and 1970 tonnes, respectively, predominantly consisting of *C. linum*, when the maximum Sc had likely not yet been reached.

In contrast, between 10 May and 7 August, the extent of meadows increased by 67%. We do not have data about the development of *R. spiralis* in recent years prior to 2021, but according to Burano Nature Oasis management (Cianchi, personal communication), the meadows had been greatly reduced and confined to small areas along the banks and at the east and west ends. This development could be attributed to the reduction in the macroalgal mat, which is a choking and competing factor towards root vegetation [43], at a time of relatively good basin environmental conditions, such as that of the early spring season, when temperatures were still sufficiently low. The rhizomes submerged in the

sediment of *R. spiralis* emit leaf shoots when the temperature exceeds 15 °C, roughly around April in the Mediterranean area [44]. However, later on, the development of *R. spiralis* was adversely affected by dystrophic conditions: by September most of the fronds and stems had detached, while by November very few clumps remained along the banks.

#### 4.5. Microphytes Blooms and the Dystrophic Event of the Second Half of August

In lagoon environments, blooms of microphytes occur when conditions become extreme, since their component species are more suitable for survival, having a very rapid turnover of life [45]. In particular, blooms of Dinophyceae occur when nutritional resources such as macromolecules and nanoparticulate are available, since this group of organisms is, for most species, mixotrophic. Their development, therefore, can be a sign of degradation of biomasses. This happened between 15 July and 7 August, when at least 600 tonnes of macroalgae decayed and blooms in isolated patches were observed.

A dystrophic condition occurred between 15 and 30 August, affecting most of the basin (Figure 6). We should speak of dystrophies, rather than a dystrophic event, since multiple events occurred in different areas, with anoxic-reducing waters that slowly mixed the entire basin. By anoxic-reducing waters, we should mean not only waters devoid of oxygen or with very low values of this gas, but the result of anaerobic processes: waters carrying reduced chemical components such as  $\text{Fe}^{\text{II}}$ ,  $\text{Mn}^{\text{II}}$ ,  $\text{S}^{2-}$ ,  $\text{S}^0$ ,  $\text{S}^{\text{IV}}$ ,  $\text{S}_2\text{O}_3^{2-}$  and  $\text{CH}_4$ , which tend to subtract oxygen coming from the atmosphere and keep these waters anoxic for a long time.

The dystrophic event was triggered due to the prevalence of very humid marine winds of intensity  $< 4 \text{ m s}^{-1}$  between 7 and 23 August. The dystrophic event continued uninterrupted until 23 August, when, following a sudden drop in temperature, conditions gradually evolved for the better, through days 30 and 31, when the acute phenomenon was considered finally over. It can be hypothesized that the development of the dystrophic phenomenon began shortly before 7 August, when the high concentration of ammonia nitrogen was evidenced, and then developed more and more until it was manifested by the formation of colloidal sulfur from day 15 onwards.

During the dystrophy, on 21 August, the survey conducted to collect physicochemical data (Table 1) showed strong lowering of DO and Eh, except for narrow areas affected by blooms of microphytes. Anoxic-reducing waters tend to evolve as they encounter oxygen, so, by taking measurements, we find a whole range of DO values in relation to the evolution of these waters. The time required for waters to evolve from extreme criticality (hydrogen sulfide release from the bottom) to acceptable conditions for life ( $\text{DO} > 1 \text{ mg L}^{-1}$ ) is variable and depends on weather conditions.

From the images related to the distribution of the dystrophic events taken by drone, the extents of the areas from which the dystrophic events sprung were identified, for the most part in areas close to the coast, which are subject to the prevailing winds that tend to accumulate biomass (Figure 6). In other more central areas, patchy dystrophic events were observed that seemed to spring from the meadows (Figure 6, lower right image). This might be surprising, since seagrass meadows are considered a key component of lagoon ecosystems [46]; in addition, they promote a state of aerobic oxidation in surface sediments due to the transport of oxygen produced by photosynthesis to the rhizosphere and the dispersal of some of this oxygen into the surrounding sediment through gaps in the root system [47] (Figure 7). Extensive uniform or patched meadows do not only have positive consequences in non-tidal lagoons. Through fronds and stems, which can reach up to the water surface, as is the case with species of the genus *Ruppia* that have anemophilous reproduction (Figure 7), they can constitute a barrier and obstacle to the circulation of water and suspended particulate matter, a kind of filter that tends to clarify water. Suspended particulate organic matter (POM), bumping against fronds and stems, tends to precipitate in and around the meadow (Figure 7). The percentage of POM in seagrass sediments often accounts for about 4% of sediment dry weight [48,49], but can be much higher in non-tidal environments (Lenzi, unpublished data). According to Danovaro [50], the origin of the

labile fraction of POM in seagrasses, derived from microphytes, is 25%. Therefore, the bottom of the meadows and surroundings tend to be enriched with organic detritus, which is labile if microphytes.

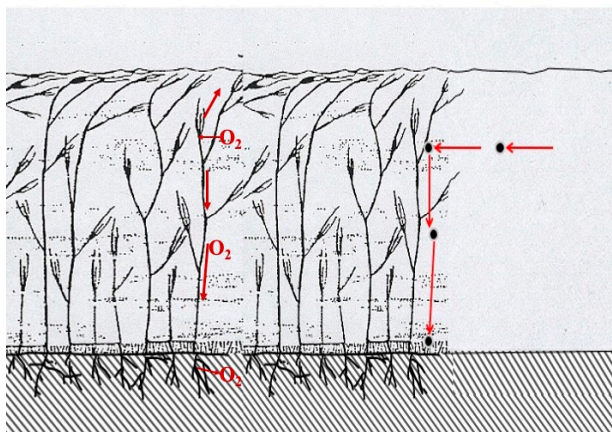


**Figure 7.** On the left, the Magnoliophyta *Ruppia spiralis* produces oxygen by photosynthesis, part of which escapes into the water column and then, for good measure, into the atmosphere, another part of which is conducted along the stem and reaches the hypogeaal apparatus, from which it can diffuse into the sediment. Dense meadows can be an impediment to water movement and particulate matter suspended in the water column, which bumps into the fronds and eventually settles around and within the meadow, enriching surface sediments of OM. On the right, a *R. spiralis* meadow has reached the surface of the water column. Thalli of the Chlorophyta *Cladophora vagabunda*, floating on the meadow, and *R. spiralis* spiral flower peduncles can be observed.

If the balance between the aerobic mineralization capacity of the meadow substrate and the amount of detritus accumulating is in favor of the former, problems do not occur, and the bottom tends to remain more or less oxidized. However, if accumulation prevails over its natural disposal (typical of eutrophic and hypereutrophic conditions), more driven anaerobic processes prevail, and localized dystrophies may occur in patches or large parts of the meadow. Under such conditions, paradoxically, the seagrass structural complex facilitates the occurrence of dystrophies; an example of this is shown in Figure 6.

Cyanobacteria blooms typically accompany and follow dystrophic events, as orthophosphate, which they require, becomes available under such conditions, while this group of bacteria is able to use diatomic nitrogen. Their development accelerates the evolution of dystrophic waters because they can produce a large amount of oxygen through photosynthesis, counteracting the anoxic-reducing condition of the waters. In the specific case of the Burano lagoon, Cyanobacteria blooms in the western part of the basin allowed the survival of a large amount of mullet that had taken refuge in that redoubt.

The mighty bloom observed in September of the Dinophyta *Alexandrium tamarense*, a species that can produce paralytic shellfish poisoning, is also to be considered a consequence of dystrophy, due to a dynamic in which opportunistic species follow one another in exploiting nutrient resources as environmental conditions change. The flagellated organisms were arranged on the water surface to catch the light, as *A. tamarense*, unlike most other Dinophyta, is not a mixotrophic species but is exclusively autotrophic. In Figure 8, an image of the bloom observed on 15 September is shown. The bloom must be related to the high availability of nutrients released by anaerobic processes, such as ammonium, nitrate and orthophosphate. Such high cell density (loss of visibility of the Secchi disk at  $-20$  cm) must be of concern for the medium term: the remains of these organisms, with a turnover that is very high, within hours or at most a few days, end up on the bottom, enriching it with LOM.



**Figure 8.** Bloom of the Dinophyta *Alexandrium tamarense* in the Burano lagoon, in September 2021.

Of course, in other lagoons and with other values of environmental variables, other opportunistic species may produce blooms after the dystrophic phenomenon, such as *Chattonella subsalsa* in Sardinia's lagoons [51] and *Gymnodinium impudicum* in the Berre lagoon [52].

Bacillariophyceae took over in November, contributing to an intense yellow-brown colouration of the waters. Diatoms are among the few organisms that can tolerate critical environmental conditions due to ammonium abundance and low oxygen. The substitution was probably induced by temperature reduction.

For the causes of such an intense dystrophic event that occurred shortly after the first half of the August, when just before the temperature was found to be lower than 28 °C, DO ranged between 3 mg L<sup>-1</sup> and 10 mg L<sup>-1</sup>, and LOM ranged between 3.96% and 8.72%, several hypotheses can be put forward. There are essentially three elements to reason about: temperature, weather conditions (also related to water dynamics) and “fuel” for the bacteria. We ascertained that the temperature increased at that time over 29 °C, high enough to promote intense bacterial activity. The weather conditions created substantial water stagnation and high air humidity, which likely reduced the nighttime exchange between the water column and the atmosphere of the heat accumulated during the day.

As for the fuel, it is possible to attribute the cause to LOM produced by the fallout of microphytes, with blooms that were observed as early as May. The microphytes consist of relatively high percentages of proteins and lipids and, thus, comprise a particularly energy-rich LOM.

Consideration could also be given to DOM in the water column, which may have provided “fuel” for SRB activity. Amino acids have also been suggested as natural substrates for SRB [53]. In May, August and November, DON constituted 89%, 68% and 51% of TDN, respectively. The trend went down over time, in conjunction with the sharp increase in ammonium. To make a rough count, which would allow an order of magnitude of the phenomenon, and taking into account only the DON, this variable was estimated as  $253.26 \pm 45.51 \mu\text{M}$  in May, corresponding to 3.545 mg L<sup>-1</sup> of N, which is equal to 22.16 mg L<sup>-1</sup> of protein in solution ( $3.545 \times 6.25$ ). In a basin of about 170 ha, with an average depth of 0.8 m ( $1.36 \times 10^9$  L), the amount of dissolved protein could have corresponded to about 30 tonnes ( $1.36 \times 10^9 \text{ L} \times 22.16 \text{ mg L}^{-1} \times 10^{-9} = 30.14$ ). This value alone

could be capable of triggering dystrophic processes in this small lagoon, the moment the environmental conditions allow it.

Then, there is the algal biomass that decayed between May and August, about 600 tonnes, corresponding to a mean value of  $1.124 \text{ kg m}^{-2}$  for the bottom area covered by macroalgae; although, this biomass was mainly made up of the decay of *C. linum*, with 40% cellulose fibres on the dried material, which are not a particularly labile matter [19]. To that should be added the biomass of *L. obscura*, which, although in relatively small amounts, consisted of more labile components.

Prospectively, a point must be made about global warming, as temperature is one of the factors driving the dystrophic process (Figure 3). Global warming is significantly affecting Western Europe and the Mediterranean basin [54,55]. Mainly, in the last thirty years, during the summer period, the subtropical desert contribution, via the African anticyclone, has been increasing, while the subtropical oceanic contribution, the Azores anticyclone, has been decreasing. The characteristics of the eastern arm of the latter have changed radically. The Azores anticyclone brought heat with dry winds from land, while the African one brings much greater heat and humid sea winds. Global warming can adversely affect lagoons, as shallow lagoon waters become loaded with thermal energy, leading to the rapid decay of plant masses and increasing the anaerobic bacteria activity. Sanz-Lazaro et al. [56], in microcosm, demonstrated that increased water temperature altered the biogeochemical cycles of sediments affected by organic matter enrichment, resulting in doubled sediment metabolism and AVS and  $\text{S}^0$  accumulation, which favors anaerobic metabolic pathways, especially sulfate respiration. In contrast, temperature increase generally selects opportunistic species that are more tolerant of warming waters, increasingly penalizing biodiversity and simplifying the food web [57]. For example, marked selection due to thermal rise has been evidenced by much work on the macroalgal populations in the Baltic Sea [58]. This means that environmental conditions in Mediterranean lagoons are likely to move increasingly towards further deterioration.

## 5. Conclusions

Non-tidal lagoons, due to their poor water exchange, morphology, structure and shallow water, tend towards eutrophication and summer criticalities, which are sometimes devastating to the biome, biodiversity, fisheries and tourism. Over the years, the strong coastal anthropization worsened this picture, increasing the frequency of criticalities and favoring the development of opportunistic species, alien or native. Dystrophic processes are the result of ecosystem degradation due to severe eutrophication. The sequence is: eutrophication, opportunistic macroalgal blooms, disappearance/reduction in seagrasses OM accumulation in the sediment and dominance of anaerobic bacterial processes; the latter involves the whole ecosystem under particular weather conditions. As the organic matter decay results in nutrient release and DOM and POM increases, blooms of opportunistic microphyte species are triggered, accompanying and facilitating the evolution of the dystrophic phenomenon.

This view of the phenomenon has not always been clear. Dystrophies become pressing and evident to people, especially when they involve fish die-offs. The causes have sometimes been attributed to one of the effects of the phenomenon, e.g., the development of a microphyte that has toxic potential, or to a complex of factors, including the loss of seagrasses, both of which are secondary phenomena. The former is a product of dystrophy, and the reduction in seagrasses, in itself, does not facilitate dystrophies but, on the contrary, is accelerated by them and, more generally, is a consequence of eutrophication.

The dystrophy of the Burano lagoon in August 2021 confirmed how these dissipative events are driven by the accumulation of organic matter, rising temperature and weather conditions favorable to the phenomenon.

To date, a prediction of the phenomenon, in time for mitigation actions, has not yet been fully achieved. It would require timely and frequent monitoring over much of a basin's surface area, capable of establishing ammonium and orthophosphate ions concentrations,

DOM loading, availability of sediment LOM and easily perishable algal masses, density of microphyte blooms and degree of sedimentation, as well as having fixed stations to record values of physicochemical variables. Continuous comparison with a weather forecasting agency would then be needed. This is a timely and complex environmental surveillance system that has never been put in place.

**Author Contributions:** M.L. and F.C. field and laboratory work and paper writing. All authors have read and agreed to the published version of the manuscript.

**Funding:** This research received no external funding.

**Institutional Review Board Statement:** The study did not require ethical approval.

**Data Availability Statement:** Original data can be obtained directly from the Authors.

**Conflicts of Interest:** The authors declare no conflict of interest.

## References

- Andersen, J.H.; Schlüter, L.; Ærtebjerg, G. Coastal eutrophication: Recent developments in definitions and implications for monitoring strategies. *J. Plankton Res.* **2006**, *28*, 621–628. [\[CrossRef\]](#)
- Hauxwell, J.; Valiela, I. Effects of nutrient loading on shallow seagrass-dominated coastal systems: Patterns and processes. In *Estuarine Nutrient Cycling: The Influence of Primary Producers*; Nielsen, S.L., Banta, G.T., Pedersen, M.F., Eds.; Kluwer Academic Publishers: Dordrecht, The Netherlands, 2004; pp. 59–92.
- Charlier, R.H.; Morand, P.; Finkl, C.W.; Thys, A. Green tides on the Brittany coasts. *Environ. Res. Eng. Manag.* **2007**, *3*, 52–59.
- Liu, F.; Pang, S.; Chopin, T.; Gao, S.; Shan, T.; Zhao, X.; Li, J. Understanding the recurrent large-scale green tide in the Yellow Sea: Temporal and spatial correlations between multiple geographical, aquacultural and biological factors. *Mar. Environ. Res.* **2013**, *83*, 38–47. [\[CrossRef\]](#)
- Grégori, G.J.; Dugenne, M.; Thyssen, M.; Garcia, N.; Nicolas, M.; Bernard, G. Monitoring of a Potential Harmful Algal Species in the Barre Lagoon by Automated in Situ Flow Cytometry. In *Marine Productivity: Perturbations and Resilience of Socio-Ecosystems*; Ceccardi, H.J., Hénocque, Y., Koike, Y., Komatsu, T., Stora, G., Tusseau-Vuillemin, M.-H., Eds.; Springer International Publishing: Berlin/Heidelberg, Germany, 2015; pp. 117–127. [\[CrossRef\]](#)
- Lenzi, M.; Leporatti-Persiano, M.; Gennaro, P. Invasive behaviour of the marine Rhodophyta *Sphaerococcus coronopifolius* Stackhouse, in a hypereutrophic Mediterranean lagoon. *Mar. Pollut. Bull.* **2022**, *181*, 113885. [\[CrossRef\]](#)
- Lenzi, M. For an Effective and Sustainable Management of Non-Tydal Lagoon Environments to Counteract the Eutrophication Effects. *Int. J. Oceanogr. Aquac.* **2021**, *5*, 11. [\[CrossRef\]](#)
- Duarte, C.M. Submerged aquatic vegetation in relation to different nutrient regimes. *Ophelia* **1995**, *41*, 87–112. [\[CrossRef\]](#)
- Lenzi, M.; Gennaro, P.; Renzi, M.; Persia, E.; Porrello, S. Spread of *Alsidium corallinum* C. Ag. in a Tyrrhenian eutrophic lagoon dominated by opportunistic macroalgae. *Mar. Pollut. Bulletin* **2012**, *64*, 2699–2707. [\[CrossRef\]](#)
- Rozan, T.F.; Taillefert, M.; Trouwborst, R.E.; Glazer, B.T.; Ma, S.; Herszage, J.; Valdes, L.M.; Price, K.S.; Luther, G.W., III. Iron-sulphur-phosphorus cycling in the sediments of a shallow coastal bay: Implications for sediment nutrients release and benthic macroalgal blooms. *Limnol. Oceanogr.* **2002**, *47*, 1346–1354. [\[CrossRef\]](#)
- Souchu, P.; Gasc, A.; Vaquer, A.; Collos, Y.; Tournier, H.; Bibent, B.; Deslous-paoli, J.M. Biogeochemical aspects of bottom anoxia in a Mediterranean lagoon (Thau, France). *Mar. Ecol. Prog. Ser.* **1998**, *164*, 135–146. [\[CrossRef\]](#)
- Cloern, J.E. Our evolving conceptual model of the coastal eutrophication problem. *Mar. Ecol. Prog. Ser.* **2001**, *210*, 223–253. [\[CrossRef\]](#)
- Giordani, G.; Azzoni, R.; Viaroli, P. A rapid assessment of the sedimentary buffering capacity towards free sulphides. *Hydrobiologia* **2008**, *611*, 55–66. [\[CrossRef\]](#)
- Amanieu, M.; Baleux, B.; Guelorget, O.; Michel, P. Etude biologique et hydrologique d'une crise dystrophique (maläigue) dans l'étang du Prevost a Palavas (Hérault). *Vie Milieu* **1975**, *XXV*, 175–204.
- Chapelle, A.; Lazure, P.; Souchu, P. Modélisation numérique des crises anoxiques (malaïgues) dans la lagune de Thau (France). *Oceanol. Acta* **2001**, *24* (Suppl. 1), 87–97. [\[CrossRef\]](#)
- Lenzi, M.; Renzi, M.; Nesti, U.; Gennaro, P.; Persia, E.; Porrello, S. Vegetation cyclic shift in eutrophic lagoon. Assessment of dystrophic risk indices based on standing crop evaluation. *Estuar. Coast. Shelf Sci.* **2013**, *132*, 99–107. [\[CrossRef\]](#)
- Cladas, Y.; Papantoniou, G.; Bekiari, V.; Fragopoulou, N. Dystrophic event in Papas lagoon, Araxos Cape, western Greece in the summer 2012. *Mediterr. Mar. Sci.* **2016**, *17*, 32–38. [\[CrossRef\]](#)
- Lenzi, M.; Persiano, M.; Gennaro, P.; Rubegni, F. Wind Mitigation Action on Effects of Eutrophication in Coastal Eutrophic Water Bodies. *Int. J. Mar. Sci. Ocean. Technol.* **2016**, *3*, 14–20.
- Sorce, C.; Persiano-Leporatti, M.; Lenzi, M. Growth and physiological features of *Chaetomorpha linum* (Müller) Kütz. in high density mats. *Mar. Pollut. Bull.* **2017**, *81*, 312–321. [\[CrossRef\]](#)

20. Preisler, A.; de Beer, D.; Lichtschlag, A.; Lavik, G.; Boetius, A.; Jørgensen, B.B. Biological and chemical sulfide oxidation in a *Beggiatoa* inhabited marine sediment. *ISME J. 1 Int. Soc. Microb. Ecol.* **2007**, *1*, 341–353. [CrossRef]
21. Lenzi, M. *Cacciatori di Solfaie. Ambienti Lagunari Atidali Eutrofici e Meccaniche Distrofiche. Hunters of SULFUR-Flows. Eutrophic Lagoon Environments and Dystrophic Mechanisms*; Pandion: Roma, Italy, 2019; 116p.
22. Rubegni, F.; Franchi, E.; Lenzi, M. Relationship between wind and seagrass meadows in a non-tidal eutrophic lagoon studied by a wave exposure model (WEMO). *Mar. Pollut. Bull.* **2013**, *70*, 54–63. [CrossRef]
23. Hamon, P.-Y.; Vercelli, C.; Pichot, Y.; Lagarde, F.; Le Gall, P.; Oheix, J. Les Malaigues de l'étang de Thau. Ome 1. Description des malaigues. Moyens de lutte, Recommandations. Ifremer, Rapport Interne, DRV/LELRL 2003-01. 2003. 65p. Available online: <https://archimer.ifremer.fr/doc/00038/14951/12277.pdf> (accessed on 11 August 2022).
24. Naqvi, S.W.A.; Bange, H.W.; Farias, L.; Monteiro, P.M.S.; Scranton, M.I.; Zhang, J. Marine hypoxia/anoxia as a source of CH<sub>4</sub> and N<sub>2</sub>O. *Biogeosciences* **2010**, *7*, 2159–2190. [CrossRef]
25. APAT; IRSA-CNR. *Metodi Analitici per le Acque*; Manuali e Linee Guida 29; IRSA-CNR: Roma, Italy, 2003; Volume 1, p. 1153. ISBN 88-448-083-7.
26. Lenzi, M.; Renzi, M. Effects of artificial disturbance on quantity and biochemical composition of organic matter in sediments of a coastal lagoon. *Knowl. Manag. Aquat. Ecosyst.* **2011**, *402*, 8. [CrossRef]
27. Loh, P.S. An Assessment of the Contribution of Terrestrial Organic Matter to Total Organic Matter in Sediments in Scottish Sea Lochs. Ph.D. Thesis, UHI Millennium Institute, Inverness, UK, 2005; 350p.
28. Schindelin, J.; Arganda-Carreras, I.; Frise, E.; Kaynig, V.; Longair, M.; Pietzsch, T.; Preibisch, S.; Rueden, C.; Saalfeld, S.; Schmid, B.; et al. Fiji: An open-source platform for biological-image analysis. *Nat. Methods* **2012**, *9*, 676–682. [CrossRef]
29. Coppejans, E. *Iconographie d'Algues Méditerranéennes. Chlorophyta, Phaeophyta, Rhodophyta*; Vaduz, C.J., Ed.; 1983; 317 planches; Available online: <https://www.worldcat.org/title/iconographie-dalgues-mediterraneennes-chlorophyta-phaeophyta-rhodophyta/oclc/647688923?referer=&ht=edition> (accessed on 11 August 2022).
30. Burrows, E.M. *Seaweed of the British Isles, V. 2 Chlorophyta*; Natural History Museum: London, UK, 1991; 238p, ISBN 0-565-00981-8.
31. WoRMS. Available online: <https://www.marinespecies.org> (accessed on 12 July 2021).
32. Ito, Y.; Ohi-Toma, T.; Nepi, C.; Santangelo, A.; Stinca, A.; Tanaka, N.; Murata, J. Towards a better understanding of the *Ruppia maritima* complex (Ruppiaceae): Notes on the correct application and typification of the names *R. cirrhosa* and *R. spiralis*. *Taxon* **2017**, *66*, 167–171. [CrossRef]
33. ICRAM. Guida al Riconoscimento del Plancton dei Mari Italiani. V. 1, Fitoplancton. Ministero dell'Ambiente della Tutela del Territorio e del Mare e Istituto Centrale per la Ricerca Scientifica e Tecnologica Applicata al Mare (ICRAM). 2006; 505p. Available online: <https://www.isprambiente.gov.it/it/pubblicazioni/manuali-e-linee-guida/guida-al-riconoscimento-del-plancton-dei-mari> (accessed on 20 September 2021).
34. ISPRA. Nuovi Approcci Metodologici per la Classificazione dello stato di Qualità Degli Ecosistemi Acquatici di Transizione. Istituto Superiore per la Protezione e Ricerca Ambientale (ISPRA) e Dip. Scienze e tecnologie Biologiche e Ambientali, Università del Salento. 2009; 108p. Available online: <https://www.isprambiente.gov.it/it/pubblicazioni/manuali-e-linee-guida/nuovi-approcci-metodologici-per-la-classificazione> (accessed on 23 August 2021).
35. Underwood, A.J. Experiments in Ecology. In *Their Logical Design and Interpretation Using Analysis of Variance*; Cambridge University Press: Cambridge, UK, 1997; Volume 12, pp. 410–411.
36. Redfield, A.C. On the proportions of the organic derivatives in sea water and their relation to the composition of plankton. In *James Johnston Memorial*; University Press of Liverpool: Liverpool, UK, 1934; pp. 176–192.
37. Atkinson, M.J.; Smith, S.V. C:N:P ratios of benthic marine plants. *Limnol. Oceanogr.* **1983**, *28*, 568–574. [CrossRef]
38. Porrello, S.; Ferrari, G.; Lenzi, M.; Persia, E. Ammonia variations in phytotreatment ponds of land-based fish farm wastewater. *Aquaculture* **2003**, *219*, 485–494. [CrossRef]
39. Caraco, N.; Cole, J.; Likens, G. Evidence for sulphate-controlled phosphorus release from sediments of aquatic systems. *Nature* **1989**, *341*, 316–318. [CrossRef]
40. Tuscany Region. Allegato 1. Prima Stesura del Piano di Sicurezza Ambientale per la Gestione della Laguna di Orbetello. Direzione Ambiente e Energia Giunta Regionale Settore Tutela Della Natura e del Mare. Delibera n.626 del 27-06-2016. Resolution of the Tuscany Regional Administration. Available online: <http://www301.regione.toscana.it/bancadati/atti/DettaglioAttiG.xml?codprat=2016DG00000000801> (accessed on 23 August 2021).
41. Danovaro, R.; Marrale, D.; Della Croce, N.; Parodi, P.; Fabiano, M. Biochemical composition of sedimentary organic matter and bacterial distribution in the Aegean Sea: Trophic state and pelagic-benthic coupling. *J. Sea Res.* **1999**, *42*, 117–129. [CrossRef]
42. Dell'Anno, A.; Mei, M.L.; Pusceddu, A.; Danovaro, R. Assessing the trophic state and eutrophication of coastal marine systems: A new approach based on the biochemical composition of sediment organic matter. *Mar. Pollut. Bull.* **2002**, *44*, 611–622. [CrossRef]
43. Hauxwell, J.; Cebrian, J.; Furlong, C.; Valiela, I. Macroalgal canopies contribute to eelgrass (*Zostera marina*) decline in temperate estuarine ecosystems. *Ecology* **2001**, *82*, 1007–1022. [CrossRef]
44. Verhoeven, J.T.A. The ecology of *Ruppia*-dominated communities in western Europe. I. Distribution of *Ruppia* representatives in relation to their autecology. *Aquat. Bot.* **1979**, *6*, 197–268. [CrossRef]
45. Platt, T.; Fillion, C. Spatial variability of the productivity: Biomass ratio for phytoplankton in a small marine basin. *Limnol. Oceanogr.* **1973**, *18*, 743–749. [CrossRef]

46. Sfriso, A.; Mistri, M.; Munari, C.; Buosi, A.; Sfriso, A.A. Management and exploitation of macroalgal biomass as a tool for the recovery of transitional water system. *Front. Ecol. Evol.* **2020**, *8*, 20. [[CrossRef](#)]
47. Pedersen, O.; Borum, J.; Duarte, C.M.; Fortes, M.D. Oxygen dynamics in the rhizosphere of *Cymodocea rotundata*. *Mar. Ecol. Prog. Ser.* **1998**, *169*, 283–288. [[CrossRef](#)]
48. Hemminga, M.; Duarte, C.M. *Seagrass Ecology*; Cambridge University Press: Cambridge, UK, 2000; 298p.
49. Enriquez, S.; Marba, M.; Duarte, C.M.; van Tussenbroek, B.I.; Reyes-Zavala, G. Effects of *Thalassia testudinum* on sediment redox. *Mar. Ecol. Prog. Ser.* **2001**, *219*, 149–158. [[CrossRef](#)]
50. Danovaro, R. Detritus–Bacteria–Meiofauna interactions in a seagrass bed (*Posidonia oceanica*) of the NW Mediterranean. *Mar. Biol.* **1996**, *127*, 1–13. [[CrossRef](#)]
51. Satta, C.T.; Padedda, B.M.; Sechi, N.; Pulina, S.; Loria, A.; Lugliè, A. Multiannual *Chattonella subsalsa* Beicheler (Raphidophyceae) blooms in a Mediterranean lagoon (Santa Giusta Lagoon, Sardinia Island, Italy). *Harmful Algae* **2017**, *67*, 61–73. [[CrossRef](#)]
52. Mayot, N.; Faure, V.; Mahé, M.; Grisel, R. An ecosystemic approach for an ecological crisis in Berre lagoon. *Vie Milieu–Life Environ.* **2020**, *70*, 77–82.
53. Takii, S. Amino acids as main substrates for sulfate reducing bacteria in surface sediment of a eutrophic bay. *J. Gen. Appl. Microbiol.* **2003**, *49*, 329–336. [[CrossRef](#)]
54. Lejeusne, C.; Chevaldonné, P.; Pergent-Martini, C.; Boudouresque, C.F.; Pérez, T. Climate change effects on a miniature ocean: The highly diverse, highly impacted Mediterranean Sea. *Trends Ecol. Evol.* **2010**, *25*, 250–260. [[CrossRef](#)]
55. Rousi, E.; Kornhuber, K.; Beodibe-Arsuag, G.; Luo, F.; Coumou, D. Accelerated western European heatwave trends linked to more-persistent double jets over Eurasia. *Nat. Commun.* **2022**, *13*, 3851. [[CrossRef](#)]
56. Sanz-Lazaro, C.; Valdemarsen, T.B.; Marin, A.; Holmer, M. Effect of temperature on biogeochemistry of marine organic-enriched systems: Implications in a global warming scenario. *Ecol. Appl.* **2011**, *21*, 2664–2677. [[CrossRef](#)]
57. Assis, J.; Bercibar, E.; Claro, B.; Alberto, F.; Reed, D.; Raimondi, P.; Serrão, E.A. Major shifts at the range edge of marine forests: The combined effects of climate changes and limited dispersal. *Sci. Rep.* **2017**, *7*, 44348. [[CrossRef](#)]
58. Takolander, A.; Cabeza, M.; Leskinen, E. Climate change can cause complex responses in Baltic Sea macroalgae: A systematic review. *J. Sea Res.* **2017**, *123*, 16–29. [[CrossRef](#)]